

Benchmarking Robustness of Deep Learning Classifiers Using Two-Factor Perturbation

Wei Dai
Department of Computer Science
Southeast Missouri State University
Cape Girardeau, MO, USA
wdai@semo.edu

Daniel Berleant
Department of Information Science
University of Arkansas at Little Rock
Little Rock, AR, USA
jdberleant@ualr.edu

Abstract— This paper adds to the fundamental body of work on benchmarking the robustness of deep learning (DL) classifiers. We innovate a new benchmarking methodology to evaluating robustness of DL classifiers. Also, we introduce a new four-quadrant statistical visualization tool, including minimum accuracy, maximum accuracy, mean accuracy, and coefficient of variation, for benchmarking robustness of DL classifiers. To measure robust DL classifiers, we created comprehensive 69 benchmarking image set, including a clean set, sets with single factor perturbations, and sets with two-factor perturbation conditions. After collecting experimental results, we first report that using two-factor perturbed images improves both robustness and accuracy of DL classifiers. The two-factor perturbation includes (1) two digital perturbations (salt & pepper noise and Gaussian noise) applied in both sequences, and (2) one digital perturbation (salt & pepper noise) and a geometric perturbation (rotation) applied in both sequences. All source codes, related image sets, and preliminary data, figures are shared on a GitHub website to support future academic research and industry projects. The web resources locate at <https://github.com/caperock/robustai>.

Keywords— Robust Deep Learning, Imperfect images, Benchmark Metrics, Corrupted images

I. INTRODUCTION

Computer scientists and engineers have innovated many benchmarking tools to measure hardware devices and compare software algorithms. Well-known, non-profit benchmark organizations include Standard Performance Evaluation Corporation (SPEC) [1], Transaction Processing Performance Council (TPC) [2], Storage Performance Council (SPC) [3], and Machine Learning Performance (MLPerf, then known as the ML Commons) [4]. These evaluate CPUs, databases, storage, and machine learning respectively. MLPerf has measured the training and inference performance of machine learning hardware, software, and services. All these organizations aperiodically update their benchmark tools, retire obsolete benchmark programs, and officially publish [results](#) on their websites.

In the machine learning field, deep learning (DL) classifiers present many unsolved challenges even though DL is one of the most hottest technologies right now. Accuracies

The authors are grateful to Google for awarding \$5,000 in cloud credits for this research.

of DL classifiers are often unstable in that they may change significantly when testing on imperfect images or adversarial attacks. DL classifiers have been shown to work well on sets of high quality images. DL classifiers have dramatically expanded in use in many scientific fields and industrial



Fig. 1. Results of SP-Gaussian corruption. The original picture is from CIFAR-10 as shown on the top left corner. (SP, GA) denotes two-factor corruption with salt & pepper noise applied first, and then Gaussian noise. (SP, GA) = (0, 0.1) indicates salt & pepper noise density is zero, but Gaussian noise density is 0.10.

projects [5][6]. For example, researchers discussed how to improve data quality via machine learning in recently reported results [7][8]. DL classifiers have classified objects in sets of high quality images at accuracy as high as 97.3%, which is better than human capabilities [9]. However, sets of low quality images present a more challenging, yet critically important, problem. If the data is imperfect, as real data so often are, how will results be affected? In [10], the researchers discovered that human visual systems are more robust than DL classifiers when images are manipulated by contrast reduction, additive noise, and distortions. In [11], DL classifier performance was lower than that of humans on recognizing images corrupted with Gaussian noise or Gaussian blur. Such limitations are a problem because, for

example, imperfect cameras sending degraded images to DL applications could result in unexpected issues. Thus, enabling DL classifiers to robustly handle imperfect images would have valuable benefits in such safety-critical application areas as unmanned vehicles, health care and life support systems [12][13].

DL classifiers can also make mistakes on apparently high quality images in the artificial intelligence security field. For example, an adversarial image may be a high quality image modified by tiny perturbations chosen to confuse DL classifiers [10] [14]-[16].

In this paper, our **contributions** are as follows:

- To measure robustness of DL classifiers, we can expect a robust DL classifier to have both high accuracy as well as low variance across the perturbation conditions. Previous scientists provided top-1 or top-5 approaches to measure accuracy. However, we define a new benchmarking methodology: we integrate mean accuracy and coefficient of variation (CV) into a two-dimensional statistical matrix for quantitatively benchmarking robustness of DL classifiers. To be best of our knowledge, this is the first research that introduce the benchmarking matrix. For details, see Eqs. 1-4.
- We provide a visualization tool named mCV plot for comparing DL classifiers. This complements the standard tools used in related work like tables, line diagrams, and bar charts. As the first study that focuses on using minimal accuracy, maximal accuracy, mean accuracy, and CV for benchmarking DL classifiers, this objective is supported by the four-quadrant mCV plot graphic. For more details, see Figs. 4-7.
- Compared with using only clean images or single factor corrupted images set, training with these two-factor perturbation image sets can improve the robustness of DL classifiers that are better than existed approaches. To be best of our knowledge, this is the first report that two-factor perturbation improves both robustness and mean accuracy of DL classifiers. For experimental results, see Table III at the end.
- Unlike previous single-factor perturbation work, two-factor perturbation provides two natural perturbations on images. The two-factor perturbation includes two digital perturbations (salt & pepper noise and Gaussian noise) applied in both orders. Also, the two-factor perturbation may consist of one digital perturbation (salt & pepper noise) and a geometric perturbation (rotation) applied in both orders. To the best of our knowledge, this is a state-of-the-art approach to measuring robustness of deep learning classifiers. We created test sets with 69 image sets. For some examples, see Figs. 1-2.
- All source codes, image sets, experimental results, and presentation videos are shared on a GitHub website to support additional research projects. For resources, see the web at <https://github.com/caperock/robustai>.

The rest of this paper is structured as follows. Section II is Related Work. In Section III, we provide the research design and methodology. Section IV introduces the experimental results. Discussion, future work, and conclusion constitute Section V, Section VI, and Section VII, respectively.

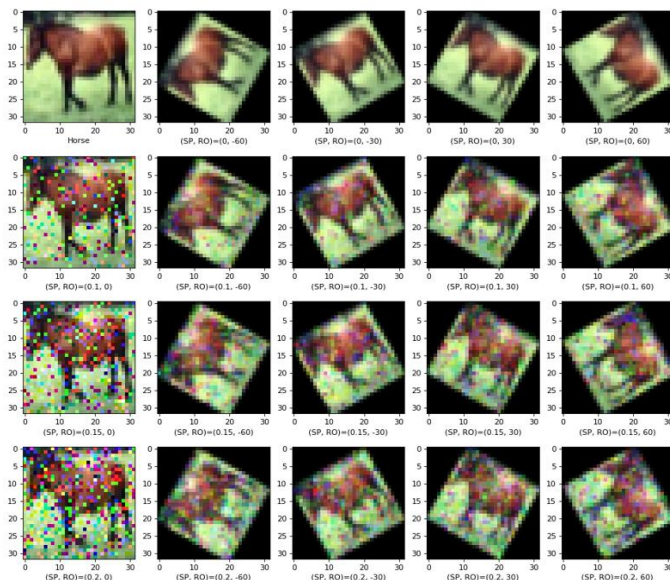


Fig. 2. Results of SP-Rotation corruption. The original picture locates at the top left corner. (SP, RO) means salt & pepper noise corruption was applied first, followed by rotation. (SP, RO) = (0.1, -30) indicates salt & pepper noise density is 0.1, and the image counterclockwise rotation was 30 degrees. (SP, RO) = (0.2, 60) indicates salt & pepper noise density is 0.2, and the image rotation is clockwise 60 degrees.

II. RELATED WORK

Researchers have discovered that DL classifiers are often fragile when faced with image perturbations. In [17], the authors demonstrated that the Google Cloud Vision API could be misled after adding approximately 14.25% impulse noise density. In [18], DL classifiers had reduced accuracy of classification when testing five types of quality distortions, including JPEG/JPEG2000 compression, blur, Gaussian noise, and contrast. There have been various previously reported corruptions imposed on high quality ImageNet datasets. In [19] the authors created 15 types of single perturbation, including Gaussian noise, blur, and brightness. In [11][20], the authors used Gaussian noise or Gaussian blur to change images. While these research projects created defective images via single factor corruptions, in the real world, image quality would often be impacted by more than one perturbation. For example, both bad weather (e.g. fog) and vibration could together impact cameras of self-driven cars, resulting in unexpected traffic accidents. In this research, we design 69 benchmarking image sets, including a clean set, sets with single factor perturbation conditions, and sets with two-factor perturbation conditions, for evaluating robustness in DL classifiers.

In addition to corruptions that involve a loss of information, vulnerable DL classifiers can also make

mistakes on adversarial corruptions in the DL security field. An adversarial picture is a high quality image modified by tiny deliberate corruptions chosen to confuse DL classifiers. Even though humans may not notice these corruptions, research shows that adversarial examples can mislead DL classifiers with deliberately modified images, leading to confused classifiers and reduced accuracy of DL classifiers [10][14]–[16].

Benchmarking metrics have many applications. Previous researchers have measured the robustness of DL classifiers via top-1 and top-5 precision analyses [21]. For example [19] chose the average rates of correct ("top-1") and almost correct ("top-5") classifications, the authors setting the top-1 error rate of AlexNet as the reference error rate. Existing results demonstrated how to utilize top-n to evaluate robustness of DL. However, we provide a two-dimensional metric, consisting of mean accuracy and coefficient of variation (CV). This supports characterizing the stability of DL classifiers as having high mean accuracy along with small CV across perturbation conditions.

The CV is the ratio of the standard deviation to the mean. The coefficient of variation is used in different fields, including physics, medicine, chemistry, and engineering [22][23]. In agriculture, Francis and Kannenberg [24] used the mean yield and coefficient of variation to analyzing yield stability. The CV offers a way to help differentiate the variation from the mean because, compared to using variance, CV controls for the mean. So, when judging a DL classifier, this article benchmarks both the mean accuracy, \bar{x} , and the coefficient of variation, CV, as they say different things. A high accuracy and small CV for a DL classifier is better than a low accuracy with a large CV because it is better on both dimensions.

III. RESEARCH DESIGN AND METHODOLOGY

A. Data processing

For measuring DL classifiers, we designed three steps: training, inference, and analysis. For details, see Fig. 3. In the training step, we used pretrained DL classifiers [26] to train and fine-tune DL classifiers. We used the Image Processing Toolbox of MATLAB 2019b for the perturbed CIFAR-10 set. Both source codes and image sets are shared on the Internet. Readers may access the GitHub resources via <https://github.com/caperock/robustai>.

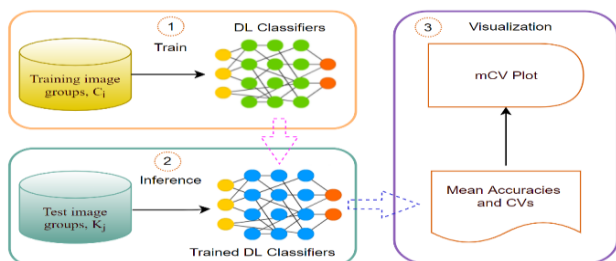


Fig. 3. An architecture for benchmarking DL classifiers. There are three steps for measuring the robustness of DL classifiers. Step 1 trains DL classifiers. Step 2 performs inference using the trained DL classifiers. Step 3 depicts the mean accuracy and coefficients of variation (CV for short) with a mCV plot.

B. Two-factor Perturbation

Previous research projects usually used single-factor corruptions on images [19][25] for benchmarking DL classifiers. For example, in [19] the authors created imperfect images through single-factor perturbations. However, images are typically impacted by multiple factors in the real world. For example, images captured by drones could be impacted by the drones' vibrations and environments such as fog or strong light. As another example, traffic signs could be faded, dirty, and/or rotated 5 or 10 degrees.

This project uses images made to be defective with two-factor perturbation. Two-factor perturbation refers to modifying images using two types of perturbation, one after the other. The two-factor perturbation may include the two digital perturbations of salt & pepper noise and Gaussian noise in different sequences. Another case of two-factor perturbation consists of a geometric perturbation (rotation) followed by a noise perturbation or noise followed by rotation.

For instance, SP-Gaussian perturbation means we firstly use salt & pepper noise for corrupting images, then use Gaussian noise for corrupting more. On the other hand, Gaussian-SP perturbation denotes changing images through Gaussian perturbation first, then applying salt & pepper perturbation. Examples of SP-Gaussian perturbation and Gaussian-SP perturbation are shown in Fig. 1. Examples of SP-Rotation perturbation and Rotation-SP perturbation are shown in Fig. 2.

The two-factor perturbation occurs in two stages. We use perturbation level and rotation ranges of [0.1, 0.2] and [-60, +60] degrees, respectively. Zero degrees denotes that we do not rotate images, negative degrees means we rotate images counterclockwise, and positive degrees means we rotate images clockwise. Specifically, two-factor perturbation types SP-Gaussian, Gaussian-SP, SP-Rotation and Rotation-SP and their ranges will be applied as shown in Table I.

TABLE I. PERTURBATION SEQUENCES, PERTURBATION TYPES, AND NOISE STRENGTHS

Perturbed Sequences	Respective Noise Strengths	
	Sequence 1	Sequence 2
SP-Gaussian	0.1, 0.15 & 0.2	0.1, 0.15 & 0.2
Gaussian-SP	0.1, 0.15 & 0.2	0.1, 0.15 & 0.2
SP-Rotation	0.1, 0.15 & 0.2	-60°, -30°, 0°, 30° & 60°
Rotation-SP	-60°, -30°, 0°, 30° & 60°	0.1, 0.15 & 0.2

C. Benchmarking Methodology

To evaluate the robustness of DL classifiers, we start with the fundamental definition that one DL classifier is more robust than another if it has higher accuracy and smaller coefficient of variation. The coefficient of variation is derived from the standard deviation (σ), which is a measure of spread of distributions in statistics. A larger σ denotes that the population of the sample data is further dispersed from the

mean. A smaller σ indicates the population of sample data is more clumped together.

In statistics, the formula for standard deviation (σ) is shown in Eq. 1.

$$\sigma = \sqrt{\frac{\sum_{i=1}^n (x_i - \mu)^2}{n}} \quad (1)$$

where x_i , n , and μ are a sample value, the number of data and the mean, respectively.

When testing performance across a group of data sets, we can collect the mean of the accuracies, μ , and the standard deviation of the accuracies, σ . We should compare the σ of different DL classifiers when their μ values are similar, because if two DL classifiers have the same mean accuracy, a smaller variation (σ) for one shows better stability in its performance across image quality conditions. We can say that a smaller variation (σ) indicates that the DL classifier performs more consistently. In brief, we want a DL classifier to have high accuracy with small standard deviation.

The coefficient of variation (or CV) denotes the standard deviation as a percentage of the mean as shown in Eq. 2.

$$CV \% = 100 \times \frac{\sigma}{\mu} \quad (2)$$

where σ is the population standard deviation, and the mean, μ , is the average of the data sets.

Unlike one-dimensional accuracy (e.g. top-1/top-5) measures of DL classifiers, we developed the mCV statistical visualization for comparing DL classifier robustness in two dimensions. We propose a four-quadrant statistical plot approach which we name the mCV (for mean accuracy and coefficient of variation) plot. See Fig. 4. In this graphical plot, the Y-axis and X-axis indicate mean accuracy and coefficient of variation, respectively. Then, the mean accuracy and CV of a reference point splits the figure into the four groups shown.

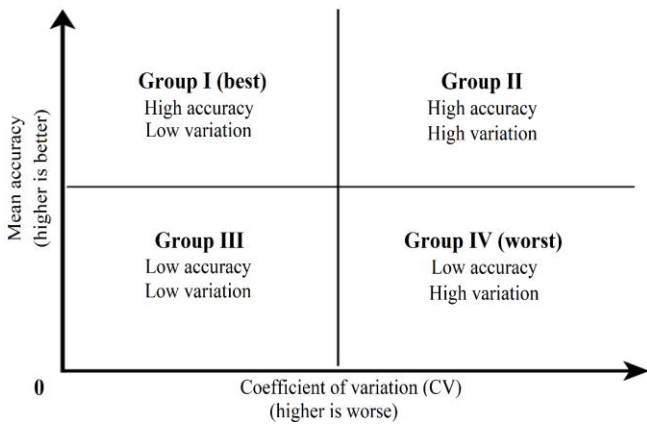


Fig. 4. Schema of mCV plots. The Y-axis and X-axis indicate mean accuracy and coefficient of variation. The mean accuracy and CV of the chosen reference point in the middle divides the above plot into four groups. It is best for a DL classifier to be in Group I.

How to split DL classifiers into the four groups is given in Algorithm 1. $Accu(clean)$ refers to the accuracy of a classifier when trained on clean images but tested on all. $CV(clean)$ refers to the coefficient of variation under the same conditions. Experimental results are shown in Figs. 5-7. In Fig. 4, $AlexNet_{clean}^{alltests}$ is the reference point. $ResNet50_{clean}^{alltests}$ and $VGG19_{clean}^{alltests}$ are the reference points in Fig. 6 and Fig. 7, respectively.

A trained DL classifier is notated as $D_{trainsets}^{testsets}$, where D refers to the DL classifier's name, testsets refers to a group of test sets, and trainsets refers to a group of training sets. Then, we test the accuracy rate on every perturbation type c . Different c values are different perturbation types, and level of severity is s , with $s \in \{0.1, 0.15, 0.2\}$ when doing salt and pepper (SP for short) or Gaussian (GA for short) perturbation. Also, $s \in \{-60^\circ, -30^\circ, 0^\circ, 30^\circ, 60^\circ\}$ when doing rotation perturbation. The accuracy rate is written $Accu(D)$ as shown in Eq. 3.

$$Accu(D)\% = 100 \times \frac{\sum_{k=1}^n Accu(D_{trainset_c}^{testset_k})}{n-1}, \quad (3)$$

where both c and k mean an image group, respectively. n is sample size. Each testing image group is listed on the GitHub website. Values for c were type 1 (clean images), type 5 (SP0.1), type 6 (SP0.1GA0.1), type 24 (GA0.1), type 25 (GA0.1SP0.1), type 43 (SP0.1RL30), type 34 (SP0.1RR30), type 40 (RL30) and type 32 (RR30). SP0.1GA0.1 means SP perturbation was applied at the 0.1 level followed by GA perturbation at the 0.1 level, respectively.

Algorithm 1: Place a DL classifier into a group in the mCV graph.

```

Input 1: MA (deep learning Mean Accuracy)
Input 2: CV (deep learning Coefficient of Variation)
Output: group number
IdentifyGroup (MA, CV){
  rMA ← mean Accu(clean)
  rCV ← CV(clean)
  if (MA ≥ rMA and CV ≤ rCV) return "Group I"
  if (MA ≥ rMA and CV > rCV) return "Group II"
  if (MA < rMA and CV ≤ rCV) return "Group III"
  if (MA < rMA and CV > rCV) return "Group IV"
}

```

For example, we can define $AlexNet_{clean}^{alltests}$ to denote the AlexNet classifier trained on a clean image set, and tested on all 69 different test image sets. $AlexNet_{SP0.1RL30}^{alltests}$ then denotes the AlexNet classifier trained on an image set corrupted by SP0.1 then corrupted more by RL30 (counterclockwise 30°).

We calculate coefficient of variation as shown in Eq. 4.

$$CV(D)\% = 100 \times \frac{\sigma}{\mu} = 100 \times \frac{\sqrt{\frac{\sum_{k=1}^{69} (Accu(D)_k - \overline{Accu(D)})^2}{n}}{\overline{Accu(D)}}} \quad (4)$$

where $CV(D)$ indicates the coefficient of variation exhibited by a DL classifier. $\overline{Accu(D)}$ denotes the mean accuracy of

the DL classifier. $Accu(\mathbf{D})_k$ indicates the accuracy of DL classifier on test set k . Variable k , $k \in [1, 69]$, is the testing image group (for more information, see the GitHub website).

The training data consists of nine training sets: a clean image set and eight corrupted image sets. Each training set has 500 images. The clean image set contains the original images. The eight corrupted image sets are corrupted according to SP0.1, GA0.1, SP0.1GA0.1, GA0.1SP0.1, SP0.1RL30, SP0.1RR30, RL30 and RR30.

Each testing set contains one clean image group and 68 corrupted image groups. The clean image group contains original images. Each testing group has 500 images. The training sets and testing sets have no overlap. In other words, if an image exists in a training set, the image will not be found in any testing set.

Abbreviated notations might not be easily read in Figs. 5-7, so we wrote labels instead. For example, the label “AlexNet(clean)” denotes the AlexNet classifier trained on the unmodified CIFAR-10 image set, but the testing was on all 69 data sets, including the clean CIFAR-10 image set and 68 corrupted versions, which we state as $AlexNet_{clean}^{alltests}$. In Table III the training data sets of CIFAR-10 are different for each row.

As shown in Fig. 5, the mean accuracy of the AlexNet(SP0.1RL30) classifier is higher (better) than AlexNet(RL30), and the CV of the AlexNet(RL30) is higher (worse) than for AlexNet(SP0.1RL30). Similarly, the minimal accuracy of AlexNet(SP0.1RL30) is higher than the minimal accuracy of AlexNet(RL30). Also, we found the same results when comparing the two maximal accuracies. However, the accuracy of AlexNet(SP0.1RL30) on uncorrupted images, 89.96% (red circle), is slightly smaller than the corresponding accuracy of AlexNet(RL30), 90.72%. For accuracy values, see Table III. The comparison is summarized visually in the mCV plot, which shows AlexNet(RL30) in Group II, while AlexNet(SP0.1RL30) is in Group I, the best quadrant because it has smaller CVs and higher mean accuracy. The mCV plot visualizes comparisons among different DL classifiers on the same test protocol.

IV. EXPERIMENTAL RESULTS

A. Benchmarking the AlexNet Classifiers on Two-factor Perturbed Images

From Table III and Fig. 5, we can see the following.

- The training datasets affected prediction CVs of the AlexNet classifiers. Notably, after training AlexNet on corrupted images, the largest CVs (with the exception of AlexNet(RR30) and AlexNet(RL30)) are less than when training is limited to clean images. The lowest accuracy are also (with the same exceptions) greater than the lowest accuracy of AlexNet trained on clean images.
- Training AlexNet on corrupted images can improve the mean accuracy during testing. Specifically, all $Accu(AlexNet_{corrupt}^{alltests})$ values are higher than

$Accu(AlexNet_{clean}^{alltests})$. AlexNet(clean) represents the AlexNet classifier trained on clean data. That is, tested accuracies tend to be better when training sets contain images that have been corrupted by degradation with common forms of noise and distortion.

- For testing on clean images, after training AlexNet on corrupted images, accuracies tend to be lower than when training AlexNet on clean images. This is intuitively unsurprising, although the difference is comparatively slight.

In brief, training AlexNet on corrupted images often improved robustness of AlexNet.

B. Benchmarking the ResNet50 Classifiers on Two-factor Perturbed Images

As shown in Table III and Fig. 6, we see the following.

- The training datasets affected prediction CVs of the ResNet50 classifiers. After training ResNet50 classifiers on corrupted images, the CVs tended to be lower (better) than after training on clean images.
- The minimum, mean and maximum accuracies, tested after training on corrupted images were lower (worse) than after training on clean images.
- As might be expected, training ResNet50 on corrupted images led to lower accuracy when tested on uncorrupted images compared to training on uncorrupted, clean images.

To sum up, training ResNet50 on corrupted images tended to improve coefficient of variation (that is, stability, in the sense of consistency of performance) of ResNet50 but reduce accuracy.

C. Benchmarking the VGG-19 Classifiers on Two-factor Perturbed Images

As shown in Table III and Fig. 7, we see the following.

- $CV(VGG-19_{clean}^{alltests})$ is greater than any $CV(VGG-19_{corrupt}^{alltests})$. This illustrates the positive effect of training on corrupted images to boost DL robustness.
- Only mean $Accu(VGG-19_{GA0.1SP0.1}^{alltests})$ is slightly higher than mean $Accu(VGG-19_{clean}^{alltests})$, while the others are lower.
- When tested on uncorrupted images, training on uncorrupted images works better than training on corrupted images.

In brief, training VGG-19 on corrupted images tends to reduce accuracy on uncorrupted images but improves coefficient of variation.

V. DISCUSSION

Experimental tests demonstrate that high accuracy of DL classifiers on high quality image sets does not ensure high stability of DL classifiers, as measured by coefficient of variation, when tested instead on images of lowered quality, which are commonly encountered in real world applications. The merged performance data of three DL classifiers with 27 training sets is shown in Table III. We conclude as follows.

- For different DL classifiers, the same corrupted image

training sets may reduce or improve the mean accuracy of DL classifiers, depending on the classifier.

- Most $CV(\mathbf{D}_{two-factor\ corrupt}^{alltests})$ values are less than the corresponding $CV(\mathbf{D}_{single\ factor\ corrupt}^{alltests})$ values. According to Table III, mean $CV(\mathbf{D}_{clean}^{alltests})$ is 2.94%; mean $CV(\mathbf{D}_{single\ factor\ corrupt}^{alltests})$ is 1.82%; mean $CV(\mathbf{D}_{two\ factor\ corrupt}^{alltests})$ is 1.42%. In other words, mean $CV(\mathbf{D}_{two\ factor\ corrupt}^{alltests})$ is somewhat better than mean $CV(\mathbf{D}_{single\ factor\ corrupt}^{alltests})$, reducing it by 0.40%. It indicates that two-factor perturbation is slightly better than single factor corruption for reducing coefficient of variation. Furthermore, this result is consistent with the increased stability (lower CV) shown by training on corrupted images.
- Comparing clean and corrupted training image sets, $Accu(\mathbf{D}_{clean}^{clean})$ is unsurprisingly above $Accu(\mathbf{D}_{corrupt}^{clean})$ for most types of corruption.
- Mean $Accu(\mathbf{D}_{clean}^{alltests})$ is 88.31%; mean $Accu(\mathbf{D}_{single\ factor\ corrupt}^{alltests})$ is 87.10%; mean $Accu(\mathbf{D}_{two\ factor\ corrupt}^{alltests})$ is 87.36%. This suggests that training on clean, single-factor corrupted, and two-factor corrupted images does not differ greatly in later mean accuracy during testing.
- Minimal $Accu(\mathbf{D}_{clean}^{alltests})$ is 85.01%; minimal $Accu(\mathbf{D}_{single\ factor\ corrupt}^{alltests})$ is 84.76%; minimal $Accu(\mathbf{D}_{two\ factor\ corrupt}^{alltests})$ is 89.57%. This shows that minimal $Accu(\mathbf{D}_{two\ factor\ corrupt}^{alltests})$ is better than $Accu(\mathbf{D}_{single\ factor\ corrupt}^{alltests})$, increasing it by 4.81%. Briefly, two-factor perturbation is the best on this question.
- Maximal $Accu(\mathbf{D}_{clean}^{alltests})$ is 92.83%, maximal $Accu(\mathbf{D}_{single\ factor\ corrupt}^{alltests})$ is 90.01%, and maximal $Accu(\mathbf{D}_{two\ factor\ corrupt}^{alltests})$ is 89.57%. To sum up, two-factor perturbation was slightly worse than single factor corruption, a result which is consistent with the increased stability of training on corrupted images.

To better understand the correlation coefficient, mean accuracy, and $Accu(clean)$ which is the accuracy when trained on clean data and tested on all data, the Spearman's rank correlation coefficient and Pearson correlation coefficient were used, as shown in Table II. Spearman's rank correlation coefficient is a statistic used for calculating the strength of a monotonic relationship between paired data (X , Y) in a sample N . Assume that a value of X has rank K and its corresponding value of Y has rank L . As shown in Eq. 5, Spearman's rank r_{xy} can be calculated for the sample data N .

$$r_{xy} = 1 - \frac{6 \sum d_{xy}^2}{n(n^2-1)} \quad (5)$$

where d is the difference between K and L , and $d_{xy}^2 = (K - L)^2$. The number of data in N is n .

The Pearson correlation coefficient is used for evaluating the strength of a linear relationship between two random

variables. The Pearson correlation coefficient, r_{xy} , can be calculated as in Eq. 6.

$$r_{xy} = \frac{\sum_i^n (x_i - \bar{x})(y_i - \bar{y})}{\sqrt{\sum_i^n (x_i - \bar{x})^2} \sqrt{\sum_i^n (y_i - \bar{y})^2}} \quad (6)$$

where x_i, y_i are paired datasets indexed with i , and \bar{x}, \bar{y} are means. The sample size is n .

From Table II, the Pearson correlation coefficients are all below 0.5. This indicates that the correlation coefficient values between CV, mean accuracy, and $Accu(clean)$ are relatively low, indicating that these three variables are at least somewhat independent.

TABLE II. SPEARMAN'S RANK & PEARSON CORRELATION COEFFICIENTS.

Data Sets	Spearman's Rank	Pearson Correlation Coefficient
CV & mean $Accu(all\ images)$	0.202	0.096
CV & $Accu(clean\ images)$	0.345	0.365
mean $Accu(all\ images)$ & $Accu(clean\ images)$	0.057	0.052

A robust DL classifier [19] [21] should produce results with high accuracies and small CVs. While accuracy and CV are, individually, one-dimensional metrics, we integrated them both into a two-dimensional metric by designing and using the mCV plot for visualizing DL classifier robustness. An advantage of the mCV plot is that it provides a visualization tool for measuring DL classifier robustness with a low learning curve. The mCV plot visualization makes the results of the present study, the first to focus on using two-factor perturbations to images for benchmarking DL classifiers, easy to compare in a convenient, understandable summarized format.

There are some potential limitations in this research. The first is the datasets. The CIFAR-10 image sets are relatively small datasets. Also, the CIFAR-10 data does not have grayscale pictures. The second limitation concerns the 68 corrupted image sets that were degraded by SP perturbations, GA perturbations, and rotations. These corrupted image sets do not constitute all types of imperfections that may distort images.

In summary, previous researchers have indicated that corrupted image sets reduce the accuracy of classifiers [18] or trigger underfit [21]. We have found that this appears to be a result of using only high quality image sets for training. As an alternative, our results indicate that it is advantageous to include corrupted image sets during training. In addition, our results were partially consistent with [18] and [21]. When testing on clean images, our results were consistent with previous researchers' reports. Nevertheless, when choosing 69 testing image sets, our results confirmed that training on defective images degraded by two-factor perturbations can enhance DL classifier robustness.

VI. FUTURE WORK

We presented an exploration of deep learning robustness under two-factor corruption. However, additional questions arise that require further research before the area could be considered fully explored. These include the following.

1) *Noise types*. This article explored two-factor perturbation with rotation, salt & pepper noise, and Gaussian noise on image sets, but other types of perturbations occur in real image processing problems and may also impact robustness of DL classifiers. Also, different image sets and diversity noise sequences, these inputting parameters may affect results.

2) *Data sets*. There are many and varied image sets on which this work might be applied and it is not known yet how well the results might generalize to data sets with different characteristics and from different domains. This remains an open question in this and many other research projects.

3) *DL Classifiers*. We tested the AlexNet, ResNet50, and VGG-19. However, DL development is a key feature of current work in the field and presents important questions related to the work we present. Certainly, a natural next step after DL benchmarking is development of new and robust DL classifiers.

4) *DL theories*. We have empirically investigated two-factor image corruption, which leads naturally to a number of “why?” questions.

- Why can training on imperfect images improve the coefficient of variation (and thus the consistency of performance) of DL classifiers?
- How can we balance the accuracy and robustness of DL classifiers?
- How can we design DL classifiers to achieve both higher accuracy and smaller CV?

Theoretical developments could suggest follow up experiments could either strengthen or weaken any proposed hypotheses.

4) *Broadened impact*. We evaluated three DL classifiers. Can the benchmarking approach and the mCV plot instead test audio data sets, numerical data, and regression and other statistical models?

5) *From 2-factor to N-factor corruption stacking*. We have claimed that 2-factor corruption better models the real world of images with their diverse imperfections. But is 2-factor image perturbation ideal, or would N -factor perturbation for some value(s) of $N \neq 2$ work better?

VII. CONCLUSION

In this research, we provided a two-dimensional metric and visualization that integrates minimal/maximal accuracy, mean accuracy, and coefficient of variation (CV), the mCV plot. This is useful for benchmarking robustness of DL classifiers. We investigated a view of robustness based on training and testing using image sets that have been deliberately corrupted to model the imperfections of images inherent in many real world applications. This study serves as a proof of concept that mean accuracy and CV can be used

together for quantitatively evaluating robustness in the performance of DL classifiers.

In this study, we tested three DL classifiers on images degraded by two-factor perturbation. The research demonstrated that training on two-factor corrupted images can slightly increase the consistency and stability of the performance of these classifiers. As a consequence, performance on the test sets for which the classifiers performed worst was generally better for classifiers trained on corrupted images than for classifiers trained on clean images. Imperfect images should certainly be considered in training, testing and benchmarking DL classifiers. In particular, any domain for which occasional poor performance should be avoided to the extent possible — even if average performance is relatively high — is a good candidate for such training. Domains of this sort would include those where even occasional cases of poor performance can be costly, such as vision systems in self-driving vehicles, detecting serious diseases in medical images, and others.

This investigation required 69 benchmarking image sets, including a clean set, sets with single factor perturbations, and sets with two-factor perturbation conditions. The datasets and source codes are publicly available as a resource for future investigations.

REFERENCES

- [1] “Standard Performance Evaluation Corporation,” SPEC. [Online]. Available: <http://www.spec.org/>.
- [2] “Transaction Processing Performance Evaluation Corporation,” TPC. [Online]. Available: <http://www.tpc.org/>.
- [3] “Storage Performance Corporation,” SPC. [Online]. Available: <http://www.spcresults.org/>.
- [4] W. Dai and D. Berleant, “Benchmarking Contemporary Deep Learning Hardware and Frameworks: A Survey of Qualitative Metrics,” 2019 IEEE First Int. Conf. Cogn. Mach. Intell., pp. 148–155, Dec. 2019.
- [5] O. Korzh, A. Sharma, M. Joaristi, E. Serra, and A. Cuzzocrea, “An Innovative Framework for Supporting Remote Sensing in Image Processing Systems via Deep Transfer Learning,” in 2020 IEEE International Conference on Big Data (Big Data), 2020, pp. 5098–5107.
- [6] N. Mo and L. Yan, “Improved faster RCNN based on feature amplification and oversampling data augmentation for oriented vehicle detection in aerial images,” *Remote Sens.*, vol. 12, no. 16, p. 2558, 2020.
- [7] W. Dai, K. Yoshigoe, and W. Parsley, *Improving data quality through deep learning and statistical models*, vol. 558. 2018.
- [8] X. Li, X. Jia, Q. Yang, and J. Lee, “Quality analysis in metal additive manufacturing with deep learning,” *J. Intell. Manuf.*, vol. 31, no. 8, pp. 2003–2017, 2020.
- [9] D. Gershgorn, “The Data That Transformed AI Research—and Possibly the World,” *Quartz*, July, vol. 26, 2017.
- [10] R. Geirhos, D. H. J. Janssen, H. H. Schütt, J. Rauber, M. Bethge, and F. A. Wichmann, “Comparing deep neural networks against humans: object recognition when the signal gets weaker,” *arXiv Prepr. arXiv:1706.06969*, 2017.
- [11] S. Dodge and L. Karam, “A study and comparison of human and deep learning recognition performance under visual distortions,” in 2017 26th International Conference on Computer Communications and Networks, ICCCN 2017, 2017.
- [12] H. Zhang, L. Cao, P. VanNostrand, S. Madden, and E. A. Rundensteiner, “ELITE: Robust Deep Anomaly Detection with Meta

- Gradient,” in Proceedings of the 27th ACM SIGKDD Conference on Knowledge Discovery & Data Mining, 2021, pp. 2174–2182.
- [13] W. Dai, “Benchmarking Deep Learning Robustness on Images with Two-Factor Corruption.” ProQuest Dissertations Publishing, Little Rock, Arkansas, 2020.
- [14] A. Kurakin, I. Goodfellow, and S. Bengio, “Adversarial machine learning at scale,” arXiv Prepr. arXiv1611.01236, 2016.
- [15] A. Madry, A. Makelov, L. Schmidt, D. Tsipras, and A. Vladu, “Towards deep learning models resistant to adversarial attacks,” arXiv Prepr. arXiv1706.06083, 2017.
- [16] N. Carlini and D. Wagner, “Adversarial examples are not easily detected: Bypassing ten detection methods,” in Proceedings of the 10th ACM Workshop on Artificial Intelligence and Security, 2017, pp. 3–14.
- [17] H. Hosseini, B. Xiao, and R. Poovendran, “Google’s cloud vision API is not robust to noise,” in Proceedings - 16th IEEE International Conference on Machine Learning and Applications, ICMLA 2017, 2018.
- [18] S. Dodge and L. Karam, “Understanding how image quality affects deep neural networks,” in 2016 eighth international conference on quality of multimedia experience (QoMEX), 2016, pp. 1–6.
- [19] D. Hendrycks and T. G. Dietterich, “Benchmarking Neural Network Robustness to Common Corruptions and Perturbations,” arXiv Prepr. arXiv1903.12261, 2019.
- [20] S. Dodge and L. Karam, “Quality resilient deep neural networks,” arXiv Prepr. arXiv1703.08119, 2017.
- [21] S. Zheng, Y. Song, T. Leung, and I. Goodfellow, “Improving the robustness of deep neural networks via stability training,” in Proceedings of the IEEE Computer Society Conference on Computer Vision and Pattern Recognition, 2016.
- [22] Y. Cohen and J. Y. Cohen, Statistics and Data with R: An applied approach through examples. 2008.
- [23] G. F. Reed, F. Lynn, and B. D. Meade, “Use of coefficient of variation in assessing variability of quantitative assays,” Clin. Diagn. Lab. Immunol., 2002.
- [24] T. R. FRANCIS and L. W. KANNENBERG, “YIELD STABILITY STUDIES IN SHORT-SEASON MAIZE. I. A DESCRIPTIVE METHOD FOR GROUPING GENOTYPES,” Can. J. Plant Sci., 1978.
- [25] I. Vasiljevic, A. Chakrabarti, and G. Shakhnarovich, “Examining the impact of blur on recognition by convolutional networks,” arXiv Prepr. arXiv1611.05760, 2016.
- [26] Chollet François, “Keras: The Python Deep Learning library,” keras.io. 2015.

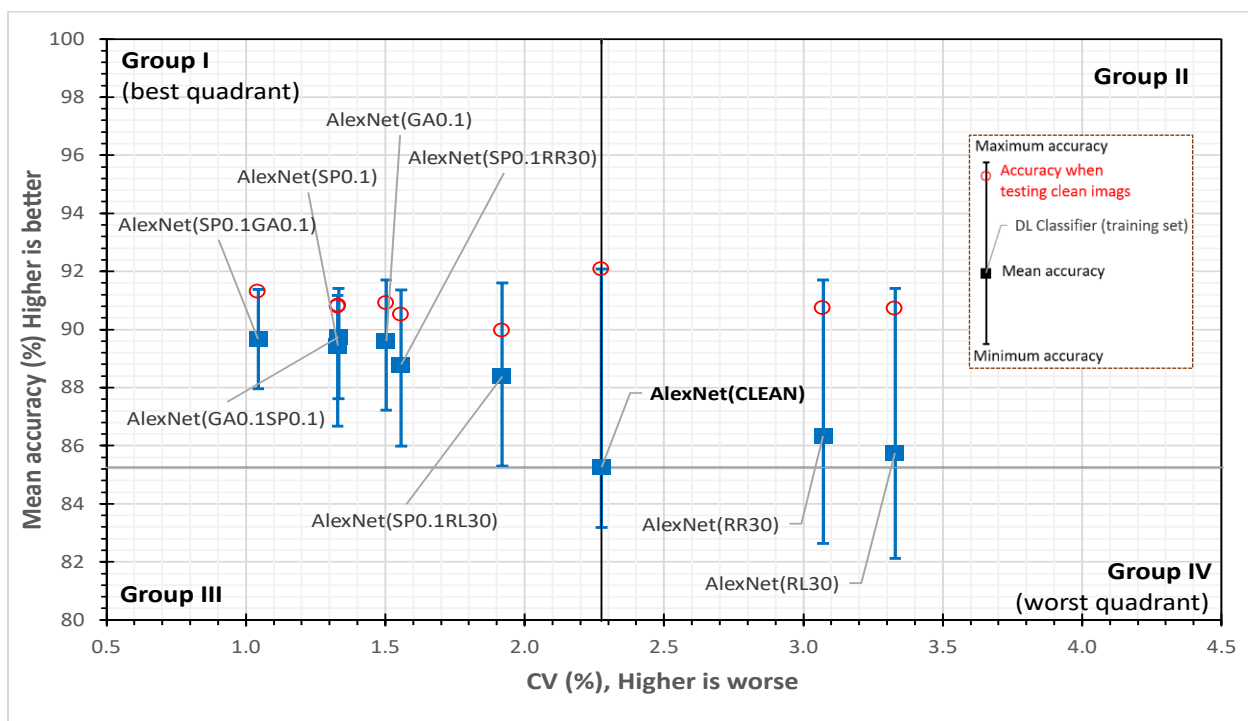


Fig. 5. The mCV plot for evaluating robustness of AlexNet classifiers after corrupted image groups were used to train the DL classifier on the CIFAR-10 dataset.

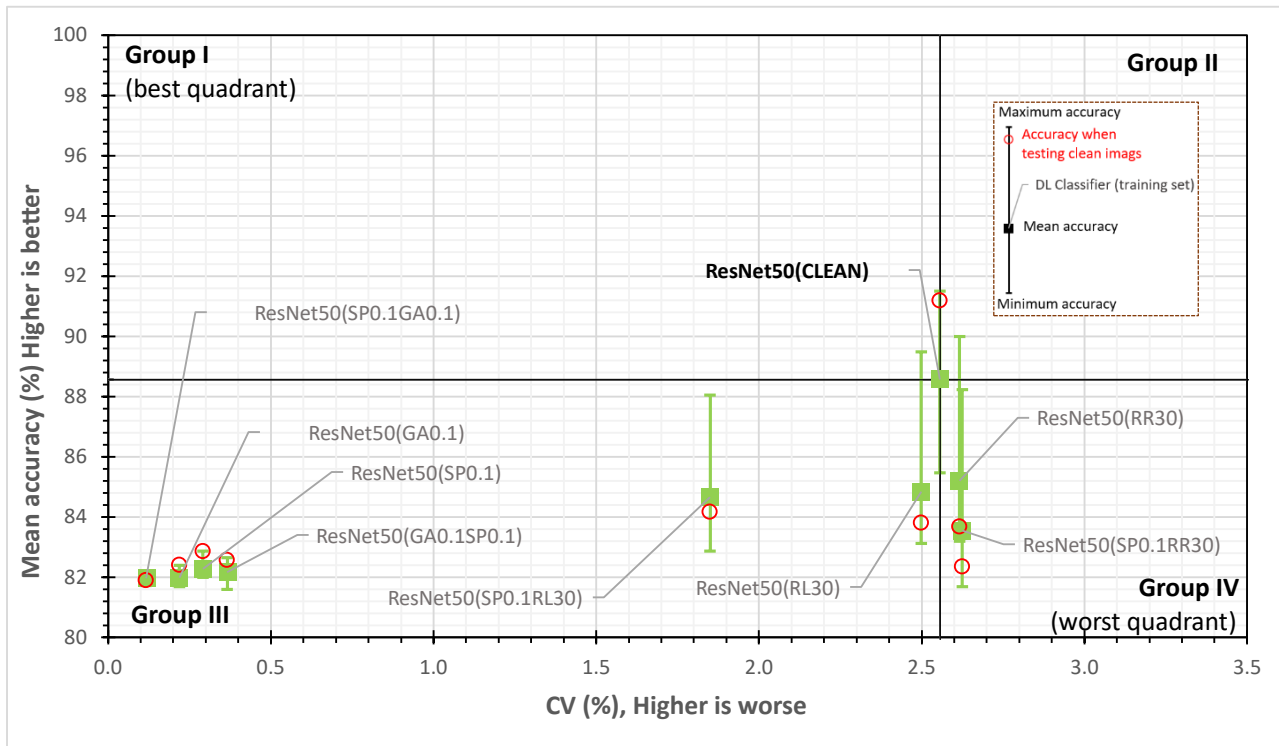


Fig. 6. The mCV plot for evaluating the robustness of ResNet50 classifiers after corrupted image groups were used to train the DL classifier on the CIFAR-10 dataset.

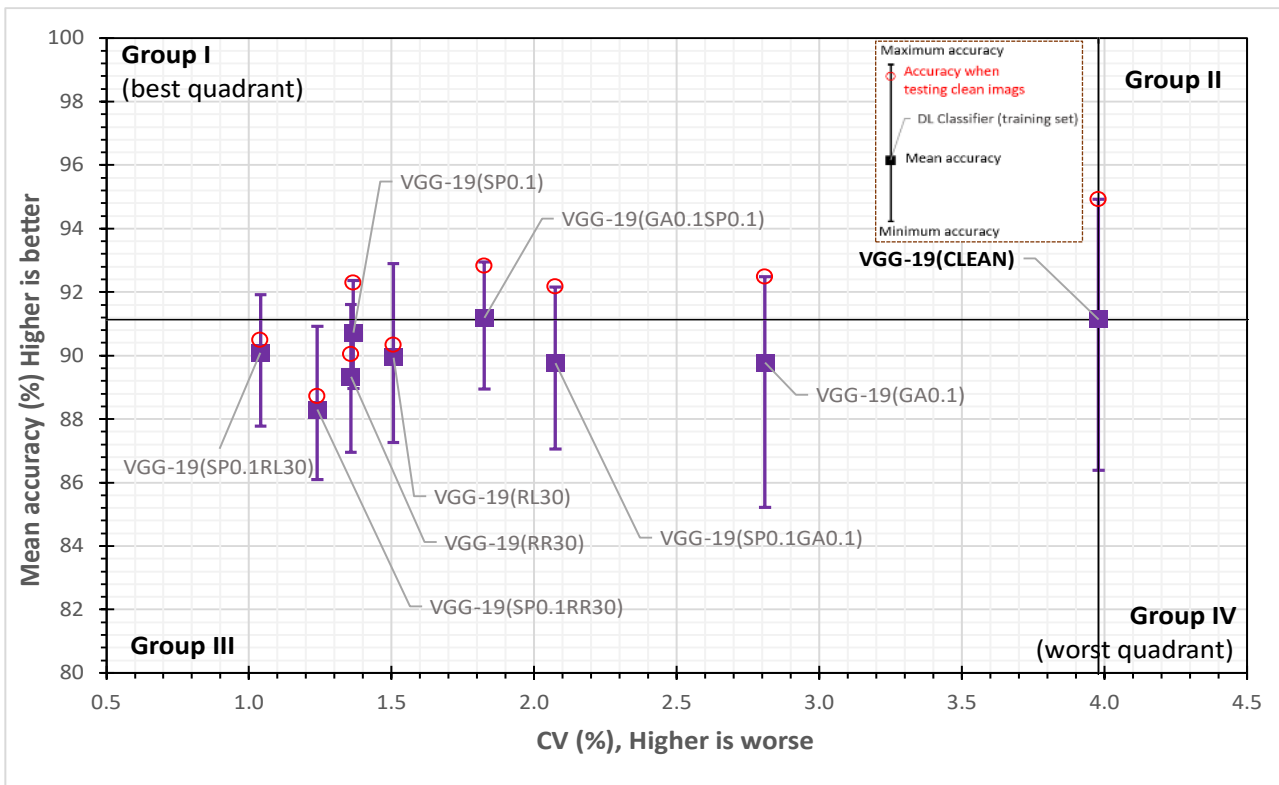


Fig. 7. The mCV plot for evaluating robustness of VGG-19 classifiers after corrupted image groups trained the DL classifier on the CIFAR-10 dataset.

TABLE III. BENCHMARKING DEEP LEARNING CLASSIFIERS WITH PERTURBATION TYPES

DL Classifier (training set)	CV (%)	Mean Accu(<i>all images</i>) (%)	Accu(<i>clean images</i>) (%)	Min Accu(<i>all images</i>) (%)	Max Accu(<i>all images</i>) (%)
AlexNet(clean)	2.28	85.25	92.08	83.18	92.08
AlexNet(GA0.1)	1.50	89.60	90.9	87.22	91.7
AlexNet(GA0.1SP0.1)	1.33	89.75	90.82	87.62	91.42
AlexNet(RL30)	3.33	85.75	90.72	82.12	91.42
AlexNet(RR30)	3.07	86.33	90.74	82.64	91.7
AlexNet(SP0.1)	1.33	89.44	90.78	86.68	91.18
AlexNet(SP0.1GA0.1)	1.04	89.67	91.3	87.96	91.38
AlexNet(SP0.1RL30)	1.92	88.39	89.96	85.3	91.6
AlexNet(SP0.1RR30)	1.56	88.79	90.52	85.98	91.36
ResNet50(clean)	2.56	88.56	91.18	85.46	91.5
ResNet50(GA0.1)	0.22	81.98	82.4	81.68	82.4
ResNet50(GA0.1SP0.1)	0.37	82.17	82.56	81.6	82.64
ResNet50(RL30)	2.50	84.83	83.8	83.12	89.48
ResNet50(RR30)	2.62	85.20	83.68	83.2	90
ResNet50(SP0.1)	0.29	82.27	82.86	82	82.86
ResNet50(SP0.1GA0.1)	0.12	81.97	81.9	81.72	82.18
ResNet50(SP0.1RL30)	1.85	84.66	84.16	82.86	88.04
ResNet50(SP0.1RR30)	2.62	83.54	82.34	81.68	88.22
VGG-19(clean)	3.98	91.13	94.92	86.38	94.92
VGG-19(GA0.1)	2.81	89.78	92.48	85.22	92.48
VGG-19(GA0.1SP0.1)	1.83	91.18	92.82	88.94	92.94
VGG-19(RL30)	1.51	89.94	90.32	87.26	92.9
VGG-19(RR30)	1.36	89.34	90.04	86.96	91.6
VGG-19(SP0.1)	1.37	90.72	92.28	88.96	92.36
VGG-19(SP0.1GA0.1)	2.07	89.77	92.16	87.06	92.16
VGG-19(SP0.1RL30)	1.04	90.08	90.48	87.78	91.92
VGG-19(SP0.1RR30)	1.24	88.30	88.72	86.1	90.92

Note that **Accu(*clean images*)** refers to training on only clean images. **Accu(*all images*)** indicates that training includes both clean images and corrupted images. For visualizing results, see Figs. 5-7.